Clinical Validation of BCI-Controlled Wheelchairs in Subjects With Severe Spinal Cord Injury

Xin Chen, Yang Yu, Jingsheng Tang, Liang Zhou, Kaixuan Liu, Ziyuan Liu, Siming Chen, Jian Wang, Ling-Li Zeng, Jinfang Liu, and Dewen Hu, *Senior Member, IEEE*

Abstract—Brain-controlled wheelchairs are one of the most promising applications that can help people gain mobility after their normal interaction pathways have been compromised by neuromuscular diseases. The feasibility of using brain signals to control wheelchairs has been well demonstrated by healthy people in previous studies. However, most potential users of brain-controlled wheelchairs are people suffering from severe physical disabilities or who are in a "locked-in" state. To further validate the clinical practicability of our previously proposed P300-based brain-controlled wheelchair, in this study, 10 subjects with severe spinal cord injuries participated in three experiments and completed ten predefined tasks in each experiment. The average accuracy and information transfer rate (ITR) were 94.8% and 4.2 bits/min, respectively. Moreover, we evaluated the physiological and cognitive burdens experienced by these individuals before and after the experiments. There were no significant changes in vital signs during the experiment, indicating minimal physiological and cognitive burden. The patients' average systolic blood pressure before and after the experiment was 113 ± 13.7 mmHg and 114 ± 11.9 mmHg, respectively (P = 0.122). The patients' average heart rates before and after the experiment were 79 ± 8.4/min and 79 ± 8.2/min, respectively (P = 0.147). The average task load, measured by the National Aeronautics and Space Administration task load index, ranged from 10.0 to 25.5. The results suggest that the proposed P300-based brain-controlled wheelchair is safe and reliable; additionally, it does not significantly increase the patient's physical and mental task burden, demonstrating its potential value in clinical applications. Our study promotes the development of a more practical brain-controlled wheelchair system.

Index Terms—Brain computer interface, brain-controlled wheelchair, cognitive burden, P300.

Xin Chen and Jinfang Liu are with the National Clinical Medical Research Center for Geriatric Diseases, and the Department of Neurosurgery, Xiangya Hospital, Central South University, Changsha, Hunan 410073, China (e-mail: jinfang_liu@csu.edu.cn).

Yang Yu, Jingsheng Tang, Kaixuan Liu, Ling-Li Zeng, and Dewen Hu are with the College of Intelligence Science and Technology, National University of Defense Technology, Changsha, Hunan 410073, China (e-mail: zengphd@nudt.edu.cn).

Liang Zhou, Ziyuan Liu, Siming Chen, and Jian Wang are with the Department of Neurosurgery, Xiangya Hospital, Central South University, Changsha, Hunan 410073, China.

I. Introduction

PARAPLEGIA caused by disease or physical injury, such as amyotrophic lateral sclerosis or spinal cord injury, is a considerable burden on patients' lives [1], [2]. The habitual behaviors of normal people, such as drinking water, are even extremely difficult for people with paraplegia [2], [3]. Brain computer interfaces (BCIs) provide a direct pathway between the user's brain and external devices without the participation of peripheral nerves and muscles; therefore, BCIs provide options for communication and control for people with neuromuscular disorders. Electroencephalogram (EEG) signals are widely used for implementing BCI systems in practical applications due to their noninvasive nature, ease of operation, and relatively low cost. Brain-controlled wheelchairs (BCWs) are a promising type of such application. Since Tanaka *et al.* developed the first EEG-based BCW system [4], many protocols have been proposed to develop a BCW [5]–[7]; these protocols have made great progress toward extending the applications of BCWs. Previous BCW systems have been extensively tested on healthy subjects in a laboratory condition [8]; however, most potential users of BCWs are people suffering from severe physical disabilities or who are in a "locked-in" state; thus, it is unclear whether these individuals could operate a BCW with brain signals as easily as healthy people. Therefore, validation of the clinical practicability of BCWs is important.

A practical BCW system should achieve its goals with less user involvement, especially when used by people with disorders, because they are more prone to fatigue. For most current BCWs, users had to control each movement of the BCWs. For example, if a user wants to take a bottle of water in a room, the user should first plan an appropriate path in mind and then control the wheelchair to move along the planned path. If there are many obstacles in the current environment, path planning is difficult. Additionally, controlling each movement of the wheelchair is burdensome and inefficient. In recent years, researchers have employed shared control techniques [9], [10]

to provide convenient and efficient strategies for controlling wheelchairs. In our previous study [11], we developed a practical BCW combining a BCI, an automatic navigation module and a computer vision (CV) module. The CV automatically perceives a dynamic environment, the user issues commands using a BCI, and the navigation module automatically controls the wheelchair to the destination. Furthermore, we installed a robotic arm on the wheelchair. If the users are interested in a target in the environment, they can select the target in the interaction interface. Next, our wheelchair automatically reaches the target and grasps the target with the robotic arm. Users do not need to spend time and energy on wheelchair navigation, which greatly improves the interaction efficiency and reduces the users' mental workload [12]–[14].

Workload could be an important issue for devices meant to be used by patients because they may exhibit a decreased capability to carry out tasks due to excessive workload required by BCIs. This, however, was only scarcely discussed in previous literature regarding BCWs. In our study, we used the National Aeronautics and Space Administration_Task Load Index (NASA-TLX) scales to measure the task workload before and after the experiment; this approach has been used in previous BCI studies [15], [16]. The NASA-TLX is divided into 6 subscales: mental demand, physical demand, temporal demand, performance, effort and frustration [17]. Each subscale has a range from 0 to 100 with a step length of 5, in which higher values indicate more workload and less user satisfaction in the specific area.

To further validate the clinical practicability of this previously proposed BCW, 10 subjects with severe spinal cord injuries were recruited for the study. The experimental results preliminarily showed the feasibility of our BCW in supplementing the motor function of patients with spinal cord injury. This experiment expanded the application of brain-computer interfaces in clinical scenarios and promoted cross-talk between neurorehabilitation and BCI research.

The rest of the paper is organized as follows. Section II describes the subjects, the structure of the BCW, the experimental procedure, and the EEG recording and decoding algorithm. Sections III and IV describe and discuss the experimental results, respectively. Finally, section V concludes our work.

II. METHODS AND MATERIALS

A. Patients

This study was approved by the Ethics Committee of Xiangya Hospital, Central South University. All processes of the study complied with the Declaration of Helsinki in 1964. The experiment was conducted at Xiangya Bo'ai Rehabilitation Hospital in Hunan Province, China. Ten patients with severe spinal cord injuries were recruited for the study. Each patient was asked to complete three experiments within one week. All patients provided signed informed consent documents. The inclusion and exclusion criteria were as described below.

The inclusion criteria were as follows: (1) age 18~70 years old; (2) muscle strength of the upper extremities lower than

TABLE I
BASIC INFORMATION OF SUBJECTS PARTICIPATING IN THE STUDY

Subjects	Sex	Age	SOSCI	Muscle strength	MMSE score
P1	Male	48	C7	2; 2-; 3; 3	29
P2	Female	54	C4	2; 2; 3; 3	29
P3	Male	56	C4	2-; 2-; 3-; 3-	22
P4	Male	40	C4	2; 1+; 3; 2	28
P5	Female	49	C4–5	2; 1+; 3; 2	29
P6	Male	25	C5	2; 1+; 3; 2	28
P7	Male	33	C4–6	2; 2; 2; 2	29
P8	Male	65	C5	2; 2; 2-; 2-	27
P9	Male	51	C4–5	2; 2; 2-; 2-	28
P10	Male	30	C4	2; 2; 3-; 3-	29

The numbers in the muscle strength column are presented in the order of "upper-left, upper-right, lower-left, lower-right". SOSCI: segment(s) of spinal cord injury. MMSE: Minimal-Mental State Examination. Muscle strength definition: level 0 refers to no muscle contraction; level 1 refers to flicker or trace of muscle contraction; level 2 refers to limb movement possible only with gravity eliminated; level 3 refers to limb movement possible against gravity but not against resistance; level 4 refers to limb movement possible against resistance with decreased power; level 5 refers to limb movement with normal power (reference: Matthews W B. Aids to the examination of the peripheral nervous system[J]. Journal of the Neurological Sciences, 1977, 33(1–2):299-299.). "+" and "-" indicate muscle strength close to but higher/lower than the given level.

level 2 and that of the lower extremities lower than level 3, secondary to various etiologies (such as trauma, stroke, and spinal injury), the definition of level 2 muscle strength refers to limb movement possible only with gravity eliminated, and level 3 refers to limb movement possible against gravity but not against resistance [18]; (3) intact consciousness (Glasgow coma scale score of 15) and reasonable cognitive function indicated by a Mini-Mental State Examination (MMSE) score >17 points for uneducated patients, >20 points for patients who only completed elementary education of fewer than 6 years, >22 points for patients who finished middle school and > 23 points for patients who finished college; also, patients should be able to comprehend the operating process of the BCW [19], [20]. (4) Finally, patients should provide signed informed consent to participate in the study (including follow-ups).

The exclusion criteria were as follows: (1) intracranial metal implants that interfere with the data acquisition of electroencephalograms; (2) history of visual defects (such as uncorrected myopia, hyperopia or astigmatism) or injury to the visual system that interferes with normal experimental process; (3) history of epilepsy; (4) unstable vital signs, including respiratory rate not within 10~24/min, systolic blood pressure not within 90~140 mmHg or pulse rate not within 60~100/min; (5) allergy to the conductive paste (GT10 medical conductive paste, GREENTEK Technological Co. ltd., Wuhan); (6) skull deformities that prevented the electrode caps from being worn continuously; (7) an unhealed wound, hemorrhage, exudation or infection of scalp; (8) pregnant women; (9) sitting position intolerance; and (10) other conditions that deemed the individual unsuitable to participate in the study.

The basic information of the patients included in the study is summarized in Table I. Eight patients were male and two were female. The average age was 45±12.7 years old. Patients suffered from spinal cord injury with the locations of the injured
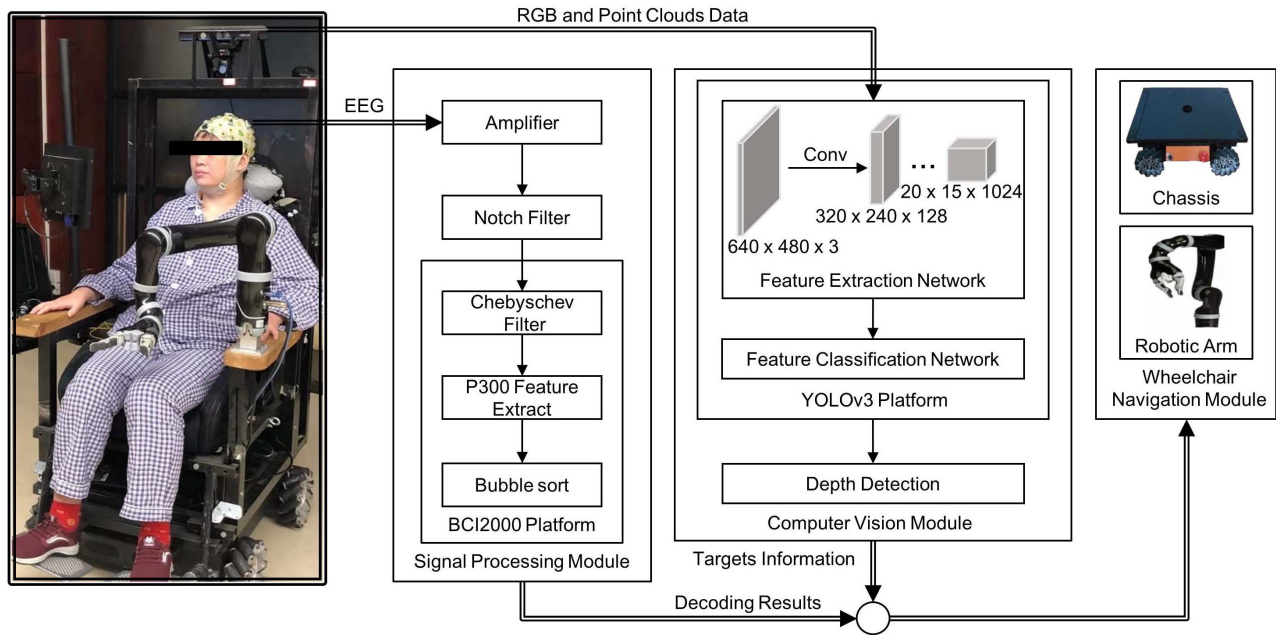
Fig. 1. The architecture of the BCW proposed in this study.

segments ranging from C4 to C7; these injuries resulted in decreased muscle strength of peripheral limbs, ranging from level 2 to level 3. The MMSE cognitive test results ranged from 22 to 29.

To ensure subject safety, vital signs, including blood pressure, heart rate and respiratory rate, were examined and recorded before and after the experiment. Before an experiment started, subject vital signs were examined and recorded, and after confirmation that these measurements were in the normal range, the experiment was initiated. After the experiment ended, the individuals' vital signs were examined again. Subjects with vital signs that were out of the normal range (indicating issues such as tachycardia or tachypnea) would receive immediate medical care provided by a doctor who accompanied the subjects.

Subjects' workloads when completing the experiment were recorded after each experiment using a self-accomplished questionnaire, the National Aeronautics and Space Administration_-Task Load Index (NASA-TLX), which contains 6 subscales, with higher values indicating higher workloads and less satisfaction. A more detailed description of NASA_TLX can be found in the introduction section. This approach has been used in previous BCI studies. The NASA-TLX is divided into 6 subscales: mental demand, physical demand, temporal demand, performance, effort and frustration. Each subscale has a range from 0 to 100 with a step length of 5, in which higher values indicate more workload and less user satisfaction in the specific area.

B. System Structure

The length, width, and height of our BCW were approximately 1.0 meters, 1.1 meters, and 1.5 meters, respectively. As shown in Fig. 1, our BCW consisted of three modules:

the signal processing module, the computer vision module, and the wheelchair navigation module. A local area network (LAN) and the transmission control protocol (TCP) were used for communication between modules.

(a) The signal processing module consisted of two submodules. The first was an amplifier (actiCHamp, Brain Products, Germany), which amplified and preprocessed the EEG signals recorded from a patient's scalp. The second was a BCI2000 platform [21] implemented on a laptop (Hasee, Hasee Computer Company, China), which extracted the P300 features and decoded the user's commands.

(b) We used a depth sensor (Kinect XBOX360, Microsoft, USA) to detect the environment in real time. The depth sensor simultaneously collected the RGB video and point cloud data. In this study, we used the YOLOv3 platform [22] to detect the environmental objects in the RGB video and then encoded the objects as the options in our BCW interface. The feature extraction network of YOLOv3 contains 53 convolutional layers and uses convolution kernels of different sizes to extract features from each frame of the captured video. The computer vision module obtained the depth information of the environmental objects from the point cloud data. The computer vision module sent the category and position of each environmental object to the wheelchair navigation module.

(c) The mecanum wheel allows translation and rotation in any direction, which is suitable for narrow indoor environments and has been widely used in BCW studies [23]. We used a chassis with four mecanum wheels to control wheelchair movement. The Kinova robotic arm (Kinova Jaco2, Kinova Robotics, Canada) had six joints and two fingers, providing it with a grasping function and six degrees of freedom [24]. The Kinova robotic arm could simulate human arms. The user interface was a computer screen with a size of approximately 1920 pixels × 1080 pixels, which showed the BCW options,
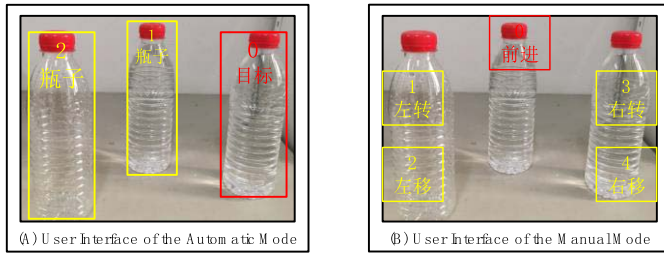
Fig. 2.   User interfaces for automatic mode and manual mode. All the patients recruited in this study were Chinese, so the options in the user interface were Chinese characters.
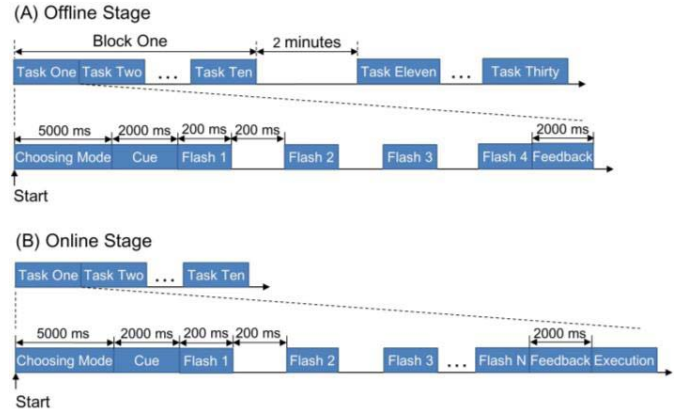

Fig. 3.   The time courses of each task. In the offline stage, each stimulus flashed four times. In the online stage, each stimulus could flash four, eight, or twelve times, and the "N" was four, eight, or twelve. In the offline stage, the time courses of each task contained 4 steps: choosing mode, cue, flash, and feedback. In the online stage, the time courses contained one more step: execution.

the stimuli used to evoke the user's P300 signals, and the decoding results. The wheelchair navigation module received environmental information from the computer vision module and received decoding results from the signal processing module. When a user selected a target, a route to the target would be automatically planned, and the BCW could go to the destination and grasp the target with the robotic arm.

The BCW we developed had two modes: automatic mode and manual mode. The subjects could change modes with a switch fixed on our BCW. In automatic mode, all BCW options were environmental objects detected by the computer vision module. Fig. 2 (A) shows the user interface for automatic mode, in which there were three options: "1 bottle", "2 bottles", and "0 target". We used a red box to mark the current target, i.e., the option "0 target". The users could select any targets in the user interface, and then the wheelchair would automatically go to the destination and grasp the target with the robotic arm. Generally, our BCW was developed for an orderly environment because paraplegic patients usually moved in such environments. If there were too many objects (set as >5) in the current environment, to avoid distracting the users' attention, the user interface only showed five of them. These five options were the five objects closest to the BCW. Fig. 2 (B) shows the user interface of the manual mode. There were five options in the user interface: "0 forward", "1 turn left", "2 move left", "3 turn right", and "4 move right". The current target was "0 forward". In this mode, the users could control each movement of the wheelchair. The interaction speed in automatic mode was high because users only needed to select targets, and the system could complete the other operations. The manual mode was useful when the users just wanted to control wheelchair movement but did not want to select any targets. With automatic mode and manual mode, our BCW might be feasible for most paraplegic patients.

C. Control Strategy for the Wheelchair And the Robotic Arm

The purpose of this study was to test the performance of our BCW in rehabilitation assistance tasks. As a preliminary case study, our control strategy was relatively simple. In this study, the BCW could detect the environment within four meters ahead. After finding the target, the wheelchair would move directly toward the target. If an obstacle was detected on the way, the wheelchair could move left and right or rotate to avoid the obstacle (the path might not be optimal).

When the wheelchair reached an area within 0.5 meters of the target, the wheelchair stopped and grasped the target with the robotic arm. Before the experiment, we needed to determine the grasping posture of the robotic arm for each target. The specific method was to manually control the robotic arm to grasp a target and then record the position of the end-effector of the robotic arm in the depth picture. The BCW would automatically build a Cartesian space, and the point in which we fixed the robotic arm was regarded as the origin of the Cartesian space. Next, the BCW system calculated the appropriate parameters to determine the grasping posture of the robotic arm for each target [9]. In the experiment, we could not interfere with the robotic arm; for example, we could not block a target when the robotic arm was grasping it.

D. Experimental Procedures

The experimental environment was a room that was approximately 8.0 meters × 9.0 meters in size. In the room, there were several human beings, bottles, chairs, and desks. For safety, the room was closed during the experiments, and no one could stay in the room except the subjects and researchers.

Each paraplegic patient participated in 3 experiments within a week. Before each experiment, subjects were told about the purposes and procedure of our experiment. We taught subjects to use our BCW and allowed subjects to try using the system until they completely understood how it worked. For safety concerns, participants' vital signs, such as blood pressure, were monitored during the experiments. Each experiment contained two stages, i.e., the offline stage and the online stage.

1) Offline Stage: In the offline stage, we needed to collect enough EEG signal data to determine the optimal parameters for the classifier. Fig. 3 shows the time courses of each task. First, the subjects were asked to select the current mode within five seconds. Then, the system displayed the corresponding user interface and reminded the subjects of the current target. Two seconds later, the user interface showed the stimuli that would evoke the subjects' P300 signals.

According to the oddball paradigm [25], the stimuli flashed with a stimulus onset asynchrony (SOA) of 400 ms, i.e., each stimulus appeared for 200 ms and disappeared for another 200 ms. In the offline stage, each stimulus flashed four times. After flashing, the classifier decoded the current result within two seconds. The BCW did not execute the decoding results but directly fed back the decoding results to the subjects through the user interface. In this study, we used the stepwise linear discriminant analysis (SWLDA) classification algorithm [26], [27]. In the offline stage, each subject had to choose 30 targets, which were divided into three blocks with ten targets in each block. To reduce the subject's mental fatigue, each subject was allowed to relax for 2 minutes after finishing each block.

2) Online Stage: In the online stage, the candidate tasks included (a) choosing bottles, chairs, people, and tables in automatic mode and (b) controlling the movement of the wheelchair in manual mode by performing forward, left turn, right turn, left translation, and right translation maneuvers. The linear velocity and angular velocity of our wheelchair are 0.08 m/s and 3.5 rad/s, respectively. For the candidate tasks in manual mode, the specific distance the forward/transaltions (cm) or turns (degrees) were decided by each subject. When a subject wanted to stop the current movement, he or she had to tell us orally, and we would stop the wheelchair. A subject could choose any candidate task, when a subject decided the task he or she wanted to do, the subject needed to tell us orally, and we would immediately record the current task. Each subject had to complete a total of ten candidate tasks in the online stage.

Here, we propose an example of how a subject could complete ten tasks. In the first task, subject X wanted to get close to a person, but the BCW did not detect the person, and subject X could not directly choose the person. Under this condition, subject X first turned left the BCW in manual mode until the BCW detected the person. Next, subject X chose the person in the automatic mode. In this study, when the BCW did not detect the target that the subject wanted to choose, the subject had to change the BCW position (by rotation or translation) before selection. Regardless of how many times the subject rotated/translated the BCW before selection, this condition was only regarded as one task. Afterward, in task 2, the subject commanded the wheelchair to turn left in manual mode, in which 13 seconds were required for decoding and 10 seconds were required to execute the turn, for a total of 23 seconds. Next, the subject moved forward in manual mode (task 3), chose a chair in automatic mode (task 4), grasped two bottles one after another with the robotic arm in automatic mode (tasks 5 and 6), and then got close to two persons one after another (tasks 7 and 8). Finally, the subject moved left (task 9) and returned to the original location (task 10). No collisions occurred during the whole process, and safety of the subject was ensured.

E. EEG Data Acquisition And Signal Processing

1) EEG Data Acquisition: According to the international 10–20 standard, we used the actiCHamp amplifier and its electrodes (Brain Products, Germany). We used five electrodes (FC1, FC2, CP1, CP2, and Cz) to record the subjects' EEG signals, two EEG electrodes (TP9 and TP10) as the reference electrodes, and Fpz as the ground electrode. The sampling frequency was 500 Hz. The impedance of all electrodes was maintained below 5 kΩ in the experiment. To reduce the electromyography (EMG) signal and electrooculogram (EOG) signal, we used a bandpass filter (0.5 Hz-50 Hz) and a zero-phase filter.

2) EEG Signal Processing: When a stimulus appeared for each option, we started recording EEG signals for 700 ms. Each 700-ms-long EEG signal contained the features of a stimulus. Next, we used a downsampling filter to filter all 700 ms-long EEG signals. The sampling rate of the downsampling filter was one tenth; in other words, we chose one point from every ten points. Therefore, the filtered signal was 70-ms-long. Then, we multiplied each 70-ms-long signal by the optimal parameter matrix W obtained by the SWLDA algorithm in the offline stage [28]. The product was the P300 score for each stimulus. In this study, multiple stimuli appeared for each option. By totalling the P300 scores of all stimuli for an option, we could obtain the P300 score of this option. Finally, we used the bubble sorting algorithm to determine the option with the maximum score, which was the decoding result.

$$S_i = \sum_{k=1}^{N} WX_{ik} \tag{1}$$

In equation (1), i is the ith option, N is the number of flashes required to decode one target, W is the optimal parameter matrix, X_{ik} is the EEG signal recorded for the ith option in the kth flash, and S_i is the P300 score of the ith option.

Decoding the subject's P300 signal was a binary classification process. The P300 classifier only needed to classify the options in the user interface as a target or nontarget [28]. As shown in equation (2), X and Y are the recorded EEG signals and the corresponding labels (target or nontarget), respectively. The SWLDA algorithm was used to determine the optimal parameter matrix W. Assuming that we collected M EEG signals with the corresponding labels in the offline experiment, X and Y could form a data set in equation (3). X_i, Y_i indicates the ith EEG signal and its corresponding label. First, the SWLDA used the linear discriminant analysis (LDA) algorithm to determine an original parameter matrix $W_{original}$ that could fit the relationship between X and Y. This process is shown in equations (4)-(7). X_{target} represents the EEG signals of the target. $\mu_{target}, \sigma_{target}$ is the mean and variance in X_{target}. For the nontargets, we calculated their mean and variance similarly according to equations (4) and (5). Then, we could calculate the divergence matrix S according to equation (6). $W_{original}$ was computed in equation (7). Next, SWLDA filtered $W_{original}$ with the stepwise regression method. This stepwise regression process was repeated until the model included a predetermined number of terms or until no additional terms satisfied the entry/removal criteria.

$$Y = WX \tag{2}$$
$$D = \left((x_1, y_1), (x_2, y_2), ..., (x_i, y_i), ..., (x_M, y_M) \right) \tag{3}$$

$$\mu_{\text{target}} = \frac{1}{N_{\text{target}}} \sum x_{\text{target}} \tag{4}$$

$$\sigma_{target} = \sum (x_{\text{target}} - \mu_{\text{target}})(x_{\text{target}} - \mu_{\text{target}})^T \tag{5}$$

$$S_W = \sigma_{\text{target}} + \sigma_{\text{non-target}} \tag{6}$$

$$W_{\text{original}} = S_W^{-1}(\mu_{\text{target}} - \mu_{\text{non-target}}) \tag{7}$$

3) Dynamic Optimization of the Number of Trials: During the online stage, the number of trials was not fixed. The system evaluates the SNR of the current P300 signals every four trials. If the SNR was greater than a predefined threshold (the maximum SNR of the subject's P300 signals recorded in the offline stage), the stimuli stopped flashing, and our BCW executed the subject's command; otherwise, each stimulus flashed four more times. In the online stage, at most, each stimulus could flash 12 times. In other words, each stimulus could flash four, eight, or twelve times. Equations (8) and (9) show the method of computing the SNR of the P300 signals [30], [31].

$$EEG_k = P300_k + Noise_k \tag{8}$$

$$SNR = 10\log_{10}\left(\frac{\text{Var}(E(EEG_k))}{E(\text{Var}(EEG_k\text{-}E(EEG_k)))}\right) \tag{9}$$

Each recorded EEG signal was composed of a noise component and a P300 component. In the two equations, k denotes the kth flash, and EEG_k is the EEG signal recorded in the kth flash. $P300_k$ and $Noise_k$ are the P300 component in the kth flash and the noise component in the kth flash, respectively. The operator E computed the mean, and$E(EEG_k)$ was the average EEG signal of all k flashes. $(EEG_k\text{-}E(EEG_k))$ reflects the noise component in the kth flash. The operator Var computed the variance. $\text{Var}(E(EEG_k)$ is the variance in the average EEG signals.

F. Performance Metrics

In this study, we used accuracy, the information transfer rate (ITR), the average number of trials, the environment detection success rate, the navigation error rate, and the average experiment time as the performance metrics. In this study, accuracy was defined as the number of successfully completed tasks divided by the total number of tasks. Successfully completing a task meant that the BCW decoded the correct target and successfully executed the subjects' commands. For example, if a subject wanted to grasp a bottle, the BCW should successfully decode the target bottle and then grasp the bottle with the robotic arm. A condition in which the BCW decoded the bottle but did not grasp it was regarded as a failure. The definition of ITR is shown in equations (10) and (11). N is the number of options in the user interface. P is the accuracy, and T is the time required to choose the current target [32], [33]. S is SOA, which was 400 ms in our experiment. R is the number of flashes required to select the current target. I is the interval between two selections. According to relevant BCI studies, one trial was defined as each option flashed once. If and only if one stimulus appeared for each option did the BCI complete a trial. For a subject, the average number of trials was the total number of trials required for this subject to complete all 30 tasks divided by 30. Additionally, each subject completed three experiments.

Every time the BCW entered automatic mode, it detected the environment. If the BCW successfully detected objects in the environment, the detection was deemed successful; otherwise, the detection was considered unsuccessful. The number of successful detections of the BCW divided by the total number of detections (number of successful detections plus the number of failed detections) was calculated as the environment detection success rate. In the experiment, an incorrect decoding of subjects' commands and an incorrect navigation of the BCW could both cause task failure. We counted the number of task failures caused by incorrect navigations. This number was divided by the total number of tasks to determine the navigation error rate. We also measured the average time that each subject required to complete an experiment.

$$ITR = \left(log_2 N + P log_2 P + (1 - P)log_2\left(\frac{1 - P}{N - 1}\right)\right)/T \tag{10}$$

$$T = (S * R + I)/60 \tag{11}$$

G. Safety Concerns

Safety and reliability were considered priorities in the design of the wheelchair. Three levels of safety guarantees were provided in the wheelchair system.

Level 1: The safety of automatic navigation system. During the navigation process of task execution, a depth camera was used to capture visual images. The navigation module of robotic operation systems is universal, and the navigation algorithm is widely used. The efficiency of the algorithm is validated to guarantee safety. Under normal conditions, no hazardous behavior is executed by the system, and the wheelchair does not collide with environmental objects.

Level 2: Ultrasonic sensors were installed around the underpan, which were not involved in route planning but were included as independent safety measures. The sensors can detect obstacles with a frequency of 20 Hz and calculate distances with an accuracy of 1 millimeter. The industrial-level high reliability PLC single chip Microco was used as the central processing unit (CPU), with a reliability higher than 99.9%. The special emergent stop module consisting of a PLC CPU and ultrasonic sensors had the highest priority among all systems, which directly controlled the electric supply. Namely, no matter what task was currently being executed, once close distance was detected by the emergent stop module, the power would be immediately cut off to ensure safety.

Level 3: A self-locking light touch switch was installed onto the underpan in an easily accessible location to meet the related safety criteria. The light touch property allows activation using only a small push. The self-locking property means that once activated, the switch requires an excessive unlocking maneuver to be performed before it is disabled, providing an additional safety measure that the switch cannot be incorrectly operated after being switched on. During each task, a safety guard would escort the person in the wheelchair and observe his or her condition. Once any condition that might be hazardous to the subject occurred, the switch was manually activated to guarantee subject safety.

TABLE II
COMPARISON OF VITAL SIGNS BEFORE AND AFTER THE TEST

Vital signs	Before the test	After the test	*P* value
SBP (mmHg)	113±13.7	114±11.9	0.122
DBP (mmHg)	77±8.1	78±7.7	0.173
HR (/min)	79±8.4	79±8.2	0.147
RR (/min)	20±1.4	20±0.8	0.921

SBP: systolic pressure; DBP: diastolic pressure; HR: heart rate; RR: respiratory rate.

Finally, clinical metrics were obtained during the experiments to ensure patient safety. Vital signs, including blood pressure, pulse rate and respiratory rate, were measured and recorded before and after each experiment to ensure that subjects maintained a proper physiological state. To assess the task load of the experiment, the NASA-TLX values before and after the experiment were recorded and analyzed.

III. RESULTS

A. P300 Signals of Subjects

P300 signals of 10 subjects are displayed in Fig. 4. All subjects demonstrated clear P300 responses. The minimal and maximal peaks of P300 signals were approximately 1 μV and 3 μV, with most peaks being approximately 2 μV. The response latencies of the subjects were approximately 200∼400 milliseconds, with a mean latency of approximately 300 milliseconds.

B. Vital Signs Before And After the Experiment

Wilcoxon rank-sum tests were applied to evaluate the difference in participants' vital signs between and after they completed the experiment, and the results are shown in Table II. The average systolic blood pressure measurements before and after the experiment were 113±13.7 mmHg and 114±11.9 mmHg, respectively. The average diastolic blood pressure measurements before and after the experiment were 77±8.1 mmHg and 78±7.7 mmHg, respectively. The average heart rates before and after the experiment were 79±8.4/min and 79±8.2/min, respectively. The average respiratory rates before and after the experiment were 20±1.4/min and 20±1.8/min, respectively. None of the vital signs demonstrated significant differences after the experiment compared with the corresponding pre-experiment values.

C. Task Load Assessment

The results of the NASA-TLX values of 10 subjects before and after the experiment are shown in Table III. The average value for each subscale ranged from 10.0 to 25.5. The maximal task load subscale was temporal load, with an average value of 25.5±2.84, while the minimal subscale was frustration, with an average value of 10.0±4.08.

D. System Performance

Subjects' performance in offline and online stages is demonstrated in Table IV. In the offline stage, the average accuracy
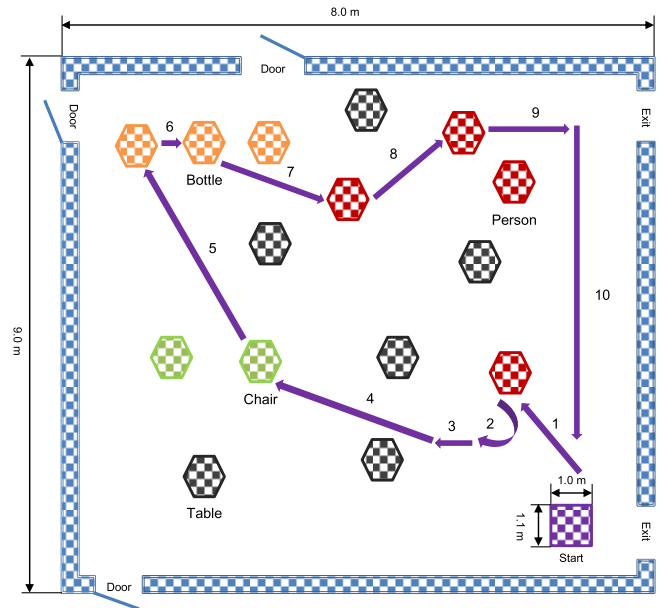

Fig. 5. Movement trajectory diagram. This figure shows the trajectory when one subject completed ten tasks. In this figure, the black, green, red, and orange polygons are tables, chairs, persons, and bottles, respectively.

and ITR were 79.2% and 5.5 bits/min, respectively. In the online stage, the average accuracy and ITR were 94.8% and 4.2 bits/min, respectively. To determine the total accuracy, i.e., the probability that the participant's order was finally fulfilled, we multiplied the environment detection success rate, the navigation success rate, and the accuracy. The average total accuracy was 90.8%. The average number of flashes in the online stage was 8 times per target, compared with 4 in the offline stage. The increased number of flashes significantly improved the classification accuracy from 79.2% to 94.8% at a minor cost of reducing the ITR from 5.5 bits/min to 4.2 bits/min, which we propose to be acceptable. The average time required to finish 10 tasks was 21.6 minutes (including intertask resting time), and the average time required to finish one task was approximately 2 minutes. The average navigation error rate was 4.5%, and the environment detection success rates of all subjects were 100%.

To further elaborate the process of executing the tasks, the process of subject 1 finishing the 10 tasks is displayed in Fig. 5 as arrowed dashed lines, and the time spent on each task is displayed in Fig. 6. In the first task, the subject headed toward a person, as indicated by the arrowed dashed line marked with number 1. Notably, 39 seconds were required to decode subject intention from the participants' P300 signals, and 15 seconds were used to execute the movement, for a total time of 54 seconds. Afterward, in task 2, the subject commanded the wheelchair to turn left, in which 13 seconds were used for decoding and 10 seconds were used to execute the turn, for a total time of 23 seconds. Next, the wheelchair headed toward a chair, after which it headed toward the bottles, grabbed the water bottles twice, and headed toward 2 persons. Finally, it returned to its original place in 2 maneuvers. No collisions
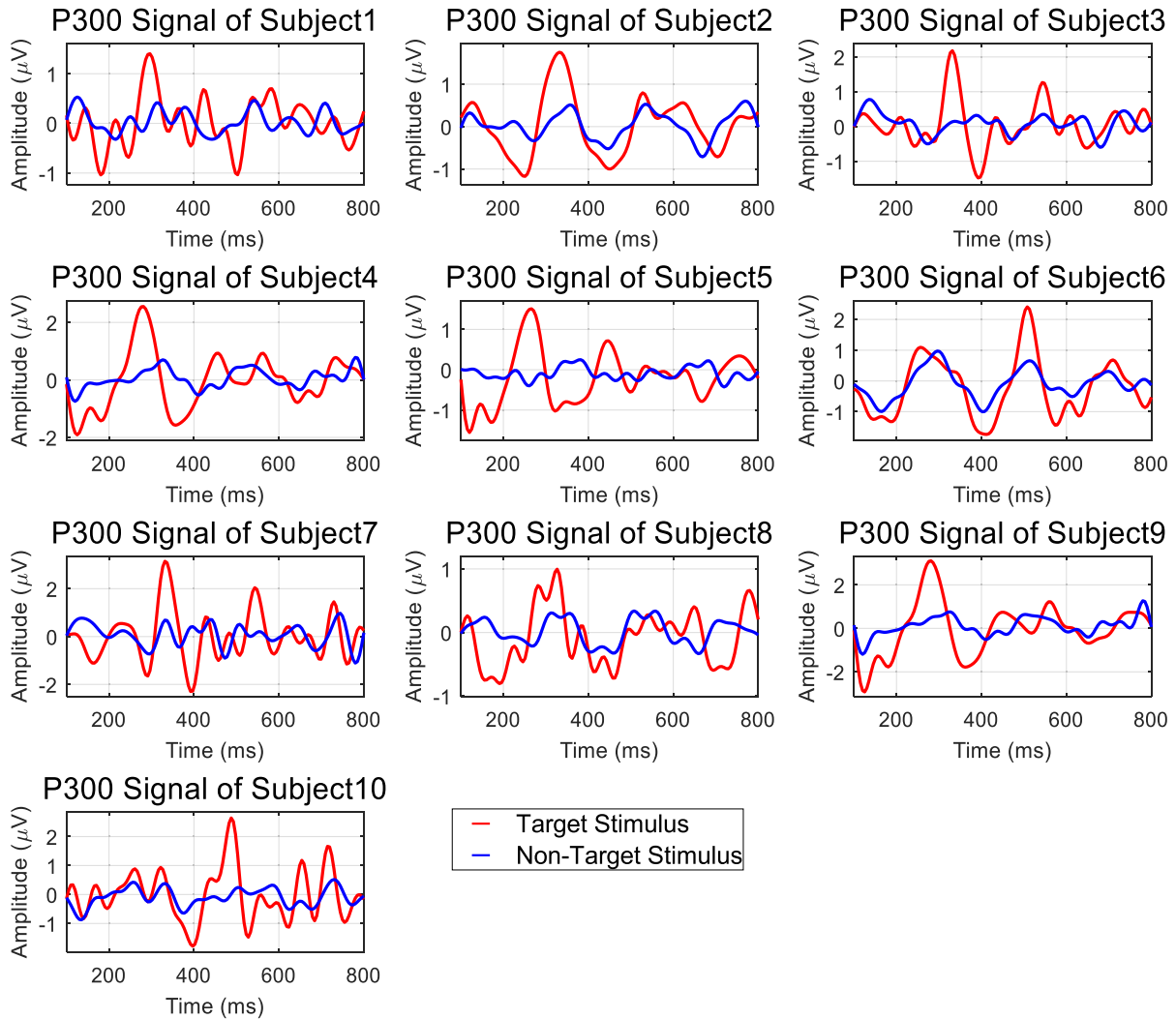
Fig. 4. P300 signals of the subjects participating in this study.

TABLE III
SCORES OF THE NASA _TLX FOR 10 SUBJECTS

Subject	Mental demand	Physical demand	Temporal demand	Performance	Effort	Frustration
P1	25	10	25	15	30	5
P2	20	15	30	10	20	10
P3	25	25	20	20	35	10
P4	40	25	25	20	25	10
P5	15	20	25	10	10	10
P6	20	20	25	15	10	10
P7	20	25	30	15	10	5
P8	35	20	25	15	25	20
P9	20	15	25	10	20	10
P10	15	25	25	15	15	10
AVG	23.5	20	25.5	14.5	20	10
STD	8.18	5.27	2.84	3.69	8.82	4.08

AVG: average; STD: standard difference.

occurred during the whole process, and safety of the subject was ensured.

IV. DISCUSSION

The average accuracy of the proposed BCW was approximately 95%, which demonstrated the feasibility of our BCW in the clinical field. The lowest accuracy of the subjects was 86.7%, which might be caused by a low state of mood.

Safety, including the stability of the physiological parameters of the subjects and the operative safety of the system, is a major concern for devices meant to be used by patients. First, we monitored participants' vital signs before and after

TABLE IV
PERFORMANCE OVERVIEW OF THE PROPOSED BRAIN-CONTROLLED WHEELCHAIR

Subject	Sex	Offline Stage		Online Stage						
		Accuracy (%)	ITR (bits/min)	Navigation success rate (%)	Environment detection success rate (%)	Average experiment time (min)	Average number of trials	Accuracy (%)	ITR (bits/min)	Total Accuracy (%)
P1	M	77.7	2.4	100	100	18.7	11.3	100	3.9	100
P2	M	80.0	5.3	90.0	100	17.0	8.3	89.7	3.9	80.7
P3	M	80.0	5.3	100	100	19.7	8.7	100	4.7	100
P4	M	100.0	10.2	90.0	100	21.7	6.4	86.7	3.7	78.0
P5	M	90.0	7.3	97.0	100	24.7	6.5	97.1	5.1	94.2
P6	M	90.0	7.3	94.0	100	22.7	7.7	93.8	4.1	88.2
P7	M	66.7	3.3	100	100	18.7	6.4	97.0	5.1	97
P8	F	65.0	3.0	100	100	23.3	7.5	100	5.2	100
P9	F	83.0	5.8	97.0	100	22.5	8.4	96.8	4.2	94.0
P10	M	60.0	4.9	87.0	100	27.3	9.1	86.7	2.9	75.4
AVG	NA	79.2	5.5	95.5	100	21.6	8.0	94.8	4.2	90.8
STD	NA	12.5	2.4	5.0	0	3.1	1.5	5.3	0.8	9.6

M: male; F: female. AVG: average; STD: standard difference; NA: not applicable.
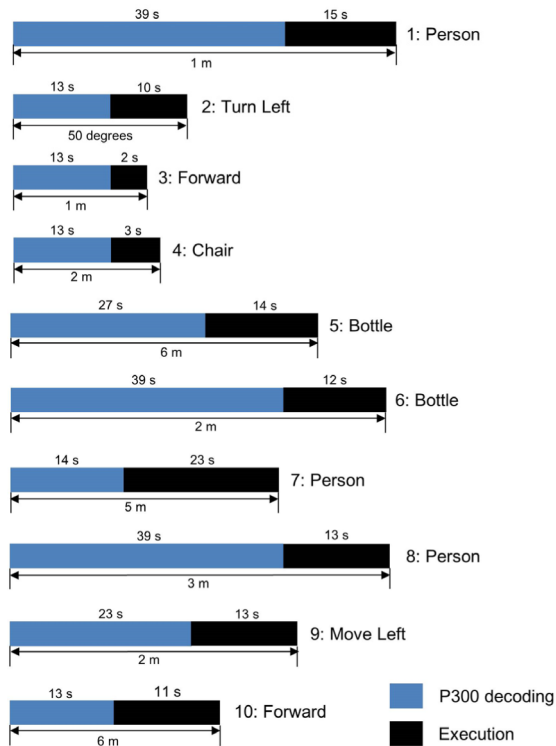

Fig. 6. Illustration of the time spent in each task. This figure shows the time spent when one subject completed the above ten tasks.

the experiment and found no significant differences. A general trend indicating physical or mental work could be raised heart rates, respiratory rates or blood pressure. The unchanged vital signs suggest that the BCW was easy to use and elicited minor physiological responses. Second, the NASA-TLX score was used to evaluate the task burden on subjects. As shown in Table III, the subscales of NASA-TLX ranged from 10.0 to 25.5, supporting the view that the cognitive burden of the system was acceptably low to allow subjects to carry out all tasks without feeling the tasks were burdensome, demonstrating clinical applicability. In addition, multiple safety guarantees were designed to ensure that the operation would not endanger the patient's safety or collide with the surrounding environment. The results showed that all subjects finished the tasks successfully.

Our BCW system could effectively help with the life of the disabled. First, it could automatically encode environmental objects, allowing subjects to directly select items as targets of interest. In addition, the route toward the target was automatically programmed, and the users did not have to control every specific movement of the wheelchair, which significantly reduced users' workload [6]. Second, direct object grasping could be achieved by the installed robotic arm, which improves the function of the wheelchair from just a platform that "moves around" and better assists disabled individuals in their daily tasks. In manual mode, the subject could also control the movement of our BCW, which was useful for cluttered environments or scenarios in which the subject just wanted to move the wheelchair. Third, the wheelchair could be controlled through visual P300 signals, which do not require limb manipulation and are easy for paraplegic patients to use. Moreover, the relatively short training time further improves the efficiency and reliability.

In this study, P300 signals were elicited through a small computer screen fixed on the BCW, and the color contrast of the screen was low, which may influence the performance of our BCW [34]. Additionally, the user interface was nonwearable, which could be uncomfortable for patients whose neck movements were restricted. Relevant studies show that using a head-mounted display (HMD) combined with augmented reality techniques (AR) might address this issue well [35]–[38]. In future work, we plan to integrate such HMDs in our BCW. Our study has several limitations. We only measured vital signs before and after the experiment, which did not guarantee the stability of vital signs during the whole process of the experiment.

V. CONCLUSION

We developed and evaluated a BCW system to help with the movements of patients with paraplegia. The system has the capability to automatically identify and encode environmental objects, perform automatic route programming and

TABLE V
TASKS PERFORMED BY EACH SUBJECT

| Subject	Task 1	Task 2	Task 3	Task 4	Task 5	Task 6	Task 7	Task 8	Task 9	Task 10
P1	Forward	Left translation	Bottle	Chair	Left turn	People	Right turn	Right translation	Bottle	Table
P2	Left turn	Left turn	Right turn	Bottle	Right translation	Bottle	Left translation	Left turn	Left turn	Right turn
P3	Forward	Left turn	Forward	Right turn	Bottle	Right turn	Right translation	Left translation	Bottle	Chair
P4	Forward	Left turn	Forward	People	Right turn	Bottle	Right turn	Bottle	Left translation	Forward
P5	Forward	Left turn	Forward	Right turn	Bottle	Left translation	Left turn	Right translation	Bottle	People
P6	Left turn	People	Forward	Bottle	Left turn	Right turn	Bottle	Left turn	Left turn	Right turn
P7	Left turn	Right turn	Left translation	Right translation	Forward	Bottle	Chair	Right turn	People	Left turn
P8	Left turn	Right turn	Right translation	Chair	Table	Bottle	Bottle	Left translation	Forward	Right turn
P9	Forward	Left translation	Bottle	Right translation	Right turn	Chair	Left translation	Table	Bottle	People
P10	Forward	Left translation	People	Bottle	Bottle	Left turn	Chair	Right turn	Left translation	Bottle
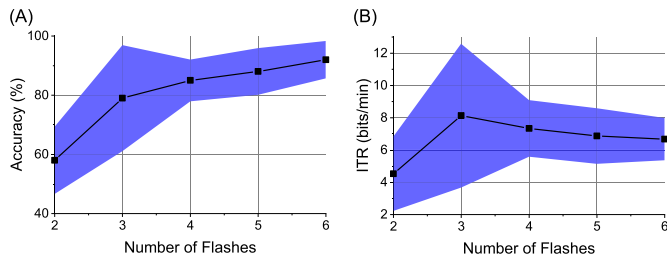
Fig. 7. The Effects of changing number of flashes. The shaded regions are the error bands.
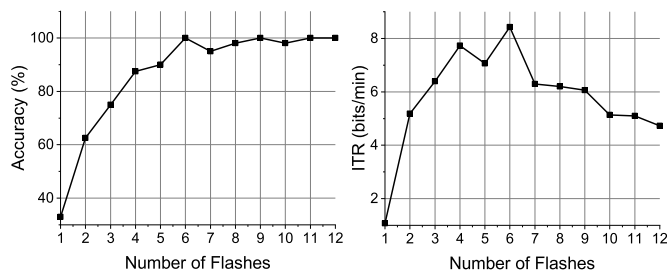

Fig. 8. Effects of changing the number of flashes on the BCW performance. This figure was plotted using the data of subject P1.

interact with environmental objects by robotic arms. The average classification accuracy was 94.8%, and the average ITR was 4.2 bits/min, with a time requirement of approximately 2 minutes for each task. No evident physiological or cognitive burdens were observed during task completion, and the users' experiences were optimal. We propose that this wheelchair system is suitable to assist the movement and environmental interaction of cognitively intact, paraplegic patients. Future work will focus on improving the system to develop a more patient-centered system and further promote its clinical applicability.

APPENDIX

See Figures 7 and 8, and see Table V.

REFERENCES

[1] D. Rosen et al., "Mutations in Cu/Zn superoxide dismutase gene are associated with familial amyotrophic lateral sclerosis," Nature, vol. 362, pp. 59–62, Mar. 1993.

[2] S. Clarke et al., "Assessing individual quality of life in amyotrophic lateral sclerosis," Qual. Life Res., vol. 10, no. 2, pp. 149–158, 2001.

[3] M. B. Bromberg, "Quality of life in amyotrophic lateral sclerosis," Phys. Med. Rehabil. Clinics North Amer., vol. 19, no. 3, pp. 591–605, 2008.

[4] K. Tanaka, K. Matsunaga, and H. O. Wang, "Electroencephalogram-based control of an electric wheelchair," IEEE Trans. Robot., vol. 21, no. 4, pp. 762–766, Aug. 2005.

[5] Y. Yu, Y. Liu, J. Jiang, E. Yin, Z. Zhou, and D. Hu, "An asynchronous control paradigm based on sequential motor imagery and its application in wheelchair navigation," IEEE Trans. Neural Syst. Rehabil. Eng., vol. 26, no. 12, pp. 2367–2375, Dec. 2018.

[6] R. Zhang et al., "Control of a wheelchair in an indoor environment based on a brain-computer interface and automated navigation," IEEE Trans. Neural Syst. Rehabil. Eng., vol. 24, no. 1, pp. 128–139, Jan. 2016.

[7] Y. Li, J. Pan, F. Wang, and Z. Yu, "A hybrid BCI system combining P300 and SSVEP and its application to wheelchair control," IEEE Trans. Biomed. Eng., vol. 60, no. 11, pp. 3156–3166, Nov. 2013.

[8] Y. Yu et al., "Self-paced operation of a wheelchair based on a hybrid brain-computer interface combining motor imagery and P300 potential," IEEE Trans. Neural Syst. Rehabil. Eng., vol. 25, no. 12, pp. 2516–2526, Dec. 2017.

[9] C. Yang, H. Wu, Z. Li, W. He, N. Wang, and C.-Y. Su, "Mind control of a robotic arm with visual fusion technology," IEEE Trans. Ind. Informat., vol. 14, no. 9, pp. 3822–3830, Sep. 2018.

[10] R. Leeb, L. Tonin, M. Rohm, L. Desideri, T. Carlson, and J. D. R. Millán, "Towards independence: A BCI telepresence robot for people with severe motor disabilities," Proc. IEEE, vol. 103, no. 6, pp. 969–982, Jun. 2015.

[11] J. Tang, Y. Liu, D. Hu, and Z. Zhou, "Towards BCI-actuated smart wheelchair system," Biomed. Eng. OnLine, vol. 17, no. 1, pp. 111–132, Dec. 2018.

[12] W. Li *et al.*, "A human-vehicle collaborative simulated driving system based on hybrid brain–computer interfaces and computer vision," *IEEE Trans. Cognit. Develop. Syst.*, vol. 10, no. 3, pp. 810–822, Sep. 2018.

[13] D. P. McMullen *et al.*, "Demonstration of a semi-autonomous hybrid brain-machine interface using human intracranial EEG, eye tracking, and computer vision to control a robotic upper limb prosthetic," *IEEE Trans. Neural Syst. Rehabil. Eng.*, vol. 22, no. 4, pp. 784–796, Jul. 2014.

[14] E. C. Tyler-Kabara *et al.*, "201 brain-machine interface control of a robotic arm for object grasping is improved with computer-vision based shared control," *Neurosurgery*, vol. 62, p. 233, Aug. 2015.

[15] Q. Huang *et al.*, "An EOG-based human–machine interface for wheelchair control," *IEEE Trans. Biomed. Eng.*, vol. 65, no. 9, pp. 2023–2032, Sep. 2018.

[16] S. He and Y. Li, "A Single-channel EOG-based Speller," *IEEE Trans. Neural Syst. Rehabil. Eng.*, vol. 25, no. 11, pp. 1978–1987, Nov. 2017.

[17] S. G. Hart and L. E. Staveland, "Development of NASA-TLX (task load index): Results of empirical and theoretical research," *Adv. Psychol.*, vol. 52, pp. 139–183, Jan. 1988.

[18] W. B. Matthews, "Aids to the examination of the peripheral nervous system," *J. Neurolog. Sci.*, vol. 33, nos. 1–2, p. 299, Aug. 1977.

[19] K. F. Kelvin *et al.*, "Cognitive tests to detect dementia: A systematic review and meta-analysis," *JAMA Internal Med.*, vol. 175, no. 9, pp. 1450–1458, 2015.

[20] R. M. Crum, "Population-based norms for the mini-mental state examination by age and educational level," *JAMA, J. Amer. Med. Assoc.*, vol. 269, no. 18, pp. 2386–2391, May 1993.

[21] G. Schalk, D. J. McFarland, T. Hinterberger, N. Birbaumer, and J. R. Wolpaw, "BCI2000: A general-purpose brain-computer interface (BCI) system," *IEEE Trans. Biomed. Eng.*, vol. 51, no. 6, pp. 1034–1043, Jun. 2004.

[22] J. Redmon *et al.*, "YOLOv3: An incremental improvement," presented at the IEEE Conf. Comput. Vis. Pattern Recognit., Salt Lake City, UT, USA, Apr. 2018.

[23] X. X. Wu, X. L. Zhang, H. D. Zhou, and W. S. Chou, "Modeling and simulation of omni-directional mobile robot with mecanum wheel," *Appl. Mech. Mater.*, vol. 624, pp. 417–423, Aug. 2014.

[24] T. M. Hemmerling, R. Taddei, M. Wehbe, C. Zaouter, S. Cyr, and J. Morse, "First robotic tracheal intubations in humans using the Kepler intubation system," *Brit. J. Anaesthesia*, vol. 108, no. 6, pp. 1011–1016, Jun. 2012.

[25] L. A. Farwell and E. Donchin, "Talking off the top of your head: Toward a mental prosthesis utilizing event-related brain potentials," *Electroencephalograph. Clin. Neurophysiol.*, vol. 70, no. 6, pp. 510–523, Dec. 1988.

[26] E. Yin *et al.*, "A novel hybrid BCI speller based on the incorporation of SSVEP into the P300 paradigm," *J. Neural Eng.*, vol. 10, no. 2, pp. 1–10, 2013.

[27] E. Yin, Z. Zhou, J. Jiang, F. Chen, Y. Liu, and D. Hu, "A speedy hybrid BCI spelling approach combining P300 and SSVEP," *IEEE Trans. Biomed. Eng.*, vol. 61, no. 2, pp. 473–483, Feb. 2014.

[28] D. J. Krusienski *et al.*, "A comparison of classification techniques for the P300 speller," *J. Neural Eng.*, vol. 3, no. 2, pp. 299–305, Dec. 2006.

[29] D. J. Krusienski *et al.*, "A comparison of classification techniques for the P300 speller," *J. Neural Eng.*, vol. 3, no. 4, p. 299, 2006.

[30] S. Lemm, G. Curio, Y. Hlushchuk, and K.-R. Müller, "Enhancing the signal-to-noise ratio of ICA-based extracted ERPs," *IEEE Trans. Biomed. Eng.*, vol. 53, no. 4, pp. 601–607, Apr. 2006.

[31] G. Pires, U. Nunes, and M. Castelo-Branco, "Comparison of a row-column speller vs. a novel lateral single-character speller: Assessment of BCI for severe motor disabled patients," *Clin. Neurophysiol.*, vol. 123, no. 6, pp. 1168–1181, Jun. 2012.

[32] X. Han, K. Lin, S. Gao, and X. Gao, "A novel system of SSVEP-based human–robot coordination," *J. Neural Eng.*, vol. 16, no. 1, Feb. 2019, Art. no. 016006.

[33] X. Chen, B. Zhao, Y. Wang, and X. Gao, "Combination of high-frequency SSVEP-based BCI and computer vision for controlling a robotic arm," *J. Neural Eng.*, vol. 16, no. 2, Apr. 2019, Art. no. 026012.

[34] C. S. Nam, Y. Li, and S. Johnson, "Evaluation of P300-based brain-computer interface in real-world contexts," *Int. J. Hum.-Comput. Interact.*, vol. 26, no. 6, pp. 621–637, May 2010.

[35] Y. Ke, P. Liu, X. An, X. Song, and D. Ming, "An online SSVEP-BCI system in an optical see-through augmented reality environment," *J. Neural Eng.*, vol. 17, no. 1, Feb. 2020, Art. no. 016066.

[36] X. Chen, X. Huang, Y. Wang, and X. Gao, "Combination of augmented reality based brain-computer interface and computer vision for high-level control of a robotic arm," *IEEE Trans. Neural Syst. Rehabil. Eng.*, vol. 28, no. 12, pp. 3140–3147, Dec. 2020.

[37] P. Arpaia, L. Duraccio, N. Moccaldi, and S. Rossi, "Wearable brain–computer interface instrumentation for robot-based rehabilitation by augmented reality," *IEEE Trans. Instrum. Meas.*, vol. 69, no. 9, pp. 6362–6371, Sep. 2020.

[38] L. Angrisani, P. Arpaia, A. Esposito, and N. Moccaldi, "A wearable brain–computer interface instrument for augmented reality-based inspection in industry 4.0," *IEEE Trans. Instrum. Meas.*, vol. 69, no. 4, pp. 1530–1539, Apr. 2020.